Research Square

Preprints are preliminary reports that have not undergone peer review.
They should not be considered conclusive, used to inform clinical practice,
or referenced by the media as validated information.

Follow the yellow flowers: remote sensing the spread of an invasive shrub in northern Patagonia

Sofía Cingolani

sofia.cingolani@comahue-conicet.gob.ar

INIBIOMA: Instituto de Investigaciones en Biodiversidad y Medioambiente https://orcid.org/0009-0001-7734-3031

Licán E. Martinez

INIBIOMA: Instituto de Investigaciones en Biodiversidad y Medioambiente

Jaime Moyano

INIBIOMA: Instituto de Investigaciones en Biodiversidad y Medioambiente

Karina L. Speziale

INIBIOMA: Instituto de Investigaciones en Biodiversidad y Medioambiente

Research Article

Keywords: spatiotemporal, sentinel–2, establishment, spread, occurrence, coverage, management

Posted Date: November 3rd, 2026

DOI: https://doi.org/10.21203/rs.3.rs-11322758/v1

License: This work is licensed under a Creative Commons Attribution 4.0 International License.
Read Full License

Abstract

Management plans to control invasive species populations require accurate distribution maps, with details on the invasion patterns and dynamics. Remote sensing is an effective tool for mapping species with distinctive spectral signatures. Cytisus scoparius is an invasive shrub that negatively affects biodiversity and ecosystem functioning in several parts of the world. In Argentina, although it was declared as a priority invasive species for control, updated information on its distribution and spread is lacking. Using the complete Sentinel–2 image series (2017–2025) we map annual invasion patterns and temporal dynamics of C. scoparius populations in Andean North Patagonia, identify drivers of occurrence and coverage, and develop spatially explicit management recommendations. We produce a high-resolution map of the invasion with a level of spatial coverage and temporal depth not achieved in earlier studies. Our findings indicate that C. scoparius population is concentrated around urban settlements, where the highest densities of the species occur, and declines toward natural areas. Temporal trend was spatially heterogeneous, where some areas gain cover while others lost it. Urban expansion was associated with cover decrease. Drivers of occurrence differed from those associated with cover: while both were mainly explained by anthropogenic and natural corridors, occurrence increased with temperature, whereas abundance increased with precipitation and had a low association with post-fire disturbance. With this information we went a step further and developed spatially explicit management strategy recommendations across the study area, presenting a practical tool for prioritizing management actions and supporting decision-making processes.

1. Introduction

The rapid increase of invasive alien species populations calls for monitoring that can rapidly detect them with effective and repeatable methods. Biological invasion is considered one of the main drivers of global change and one of the major causes of species extinction (IPBES, 2019) promoting the homogenization of the world's flora and fauna (Mooney & Hobbs, 2000). As invasive populations spread, they can alter the spatial configuration of vegetation, resulting in distinct patches that contrast with the surrounding native vegetation. This contrast is key for detecting and mapping their distribution and dynamics over time. Such information can further help identify areas where management actions are most needed and support more effective allocation of resources, as prioritization usually requires understanding the extent to which different factors influence where species establish and how they spread across landscapes (Trueman et al. 2014; Carter et al. 2024).

Landscape features associated with human activity and anthropogenic or natural disturbance often generate suitable environmental conditions for invasion (Aranda et al. 2024), in combination with favorable species-specific climatic and topographic factors. At global scale, urban areas harbor a larger proportion of alien plant species than surrounding natural ecosystems, mainly due to repeated human-mediated introductions and the creation of novel environmental conditions that facilitate invasion (Potgieter & Cadotte 2020; Potgieter et al. 2024). Likewise, linear landscape features such as roads, rivers and lake shores influence invasion patterns by increasing landscape connectivity and enabling

both local spread and long distance dispersal events (Haubrock et al. 2026). In addition, many of these features are subjected to recurrent disturbances that reduce competition and increase resource availability that invasve species benefit from (Davis et al. 2000). Other kind of disturbance events, such as wildfires, may alter habitat conditions and create opportunities for population expansion (Brooks et al. 2004; Meyer et al. 2021). Understanding how these factors influence invasion requires spatially explicit evidence of the species distribution and dynamics, which is also essential to support management decisions.

The design of efficient management plans for invasive populations requires accurate distribution maps, with details on the intensity of the invasion and its spatial pattern over time, particularly given funds for control of invasive species are often scarce (Trueman et al. 2014). While most studies center their attention on species occurrence data because it provides direct information on establishment, information on the spatial extent and configuration of invasive populations is less frequently available, despite being essential for understanding population dynamics through growth and spread (Bradley et al. 2018; O'Neill et al. 2021). Moreover, the factors that determine occurrence are not necessarily the same as those influencing spatial extent and configuration (O'Neill et al. 2021). In this sense, remote sensing is an effective tool for mapping invasive vegetation in an exhaustive way (Franklin, 2010; Hill et al. 2016). However, most applications remain constrained by one or more limitations, including short temporal records and little attention to long-term invasion dynamics, relatively small spatial extents or limited transferability across regions (Bolch et al. 2020; Walsh 2018). Nevertheless, continuous improvements in the spatial, spectral and temporal resolution of satellite imagery and current availability of medium to high resolution imagery have substantially enhanced the accuracy and reliability of mapping individual invasive plant species according to its spectral properties (Lamb and Brown, 2001; Boyle et al. 2014).

There are a few essential characteristics that determine whether a single species population can be mapped. First, differences in spectral reflectance or texture between the species of interest and the rest of the vegetation must be contrasting (Lamb and Brown, 2001). Particular spectral characteristics can be obtained by a combination of several features visible in the spatial or temporal extent, for example, whether the plant forms a particular tree crown, high foliage density or visible phenology changes (Carrión-Klier et al. 2022; Bolch et al. 2020). Also, for the satellite to detect the species, it must be the dominant species over the canopy and its occupation must form a monospecific stand larger than the resolution of the satellite (Lamb and Brown, 2001).

The invasive shrub *Cytisus scoparius* (L.) Link (locally known as retama or scotch broom), a perennial legume native to Europe, could be a good candidate for satellite detection. This invader usually forms large monospecific stands with massive flower blooms (Cavallero et al. 2018). Individuals can achieve reproductive maturity at 3–5 years, when they produce several thousand of bright-yellow flowers that bloom relatively synchronously (Parker, 1997). After this period, its pollinated flowers become a black legume-type fruit, losing the strong yellow color of the patch and thus, becoming more similar to the surrounding vegetation. In the southern hemisphere, flowering typically occurs from November to

December and lasts approximately 4–8 weeks, depending on environmental conditions (Parker 2000; Stout 2000). The longevity of the flowering period can be shortened by the effects of wind, rain, temperature, and grazing by insects during pollination (Hill et al. 2016). By using a sufficiently wide time range, satellite images can detect the patches despite variation of these factors (Carrión-Klier et al. 2022). Another advantage for detecting *C. scoparius* population with remote sensing is that most occurrences are expected to be in the open and visible areas, because it is often an early colonizer (Hosking et al. 1996) and mostly shade intolerant (DiTomaso, 1998). Although a recent study assessed different aspects of its establishment along roadsides of Nahuel Huapi National Park (Montero-Castaño et al. 2023), there is not specific information of its total distribution, rate of spread, new spread locations, and overall extent of the problem in Northern Patagonia. While this approach has proven to be efficient with invasive *C. scoparius* populations of southwest Canada (Hill et al. 2016), no previous study has assessed temporal dynamics of its distribution. On the other hand, advances in satellite technology over the past decade and better resolution images availability now allow the generation of more detailed and accurate maps (Phiri et al. 2020), facilitating the identification of the main drivers of invasive *C. scoparius* occurrence and spread and the identification of areas that could be prioritized for management.

In this study, we aimed to assess the spatiotemporal dynamics of *C. scoparius* invasion across northern Patagonia using high-resolution Sentinel-2 imagery, identify the main drivers behind the spread of this invader and identify spatially explicit priority areas for management. Specifically, we quantified changes in invasion extent from 2017 to 2025 using the complete Sentinel-2 image archive available for this period, providing one of the longest satellite-based regional assessments of an invasive plant conducted in South America. Our specific objectives were: (1) produce one map for each year of *C. scoparius* invasion and quantify spatially if its distribution grew or declined, (2) evaluate how topographic (elevation), climatic (temperature, precipitation), disturbance (wildfire), landscape features (roads, rivers, lake shores) and land use (urban settlements, national parks) factors influence the species occurrence and invasion extent, (3) characterize the size and spatial configuration of *C. scoparius* invasion patches and identify areas of management priority to support stakeholders with spatially informed management decisions. Given that this invasive species is recognized as problematic and needs to be removed to reduce its negative impacts (Administración de Parques Nacionales, 2007; Boletín Oficial de la República Argentina, 2021), we expect our methodology will serve as baseline for management planning, not only for the study area but to be applied to similar situations in other parts of the world that suffer from problems with invasive species populations with identifiable spectral characteristics.

2. Material and Methods

2.1. Study Area

The study area was located in northern Patagonia in an approximated area of 2,400,000 ha (2,469,653 ha) corresponding to the eastern foothills of the Andes mountain range (Fig. 1). The area spans approximately 450 km from north to south (38°50'–43°56' S) and ranges from 200-3700 m a.s.l.,

bounded between the limits of two National Parks, the Lanin north border and Los Alerces south border, having as its western limit the border with Chile and to the east the phytogeographic limit where the Andean forest meets the steppe (according to Oyarzabal et al. 2018) slightly expanded to include nearby towns with a record of invasion by the species.

We selected this area because it encompasses four National Parks that had reported their concern about *C. scoparius* invasion. Also, because it presents the highest density of *C. scoparius* observations in Argentina (iNaturalist). In addition, its vegetation shares similar phytogeographic units, dominated by humid forest and shrublands, to which a single satellite mapping technique can be applied.

2.2. Study species

Cytisus scoparius is native to Europe and has been introduced as ornamental in several parts of the world becoming a vigorous invader (Prasad, 2005; Zouhar, 2005). In Argentina, it became naturalized in the Patagonian Region, near the Andes mountain range, from Neuquén province to almost the southern limit of Santa Cruz province. This species is considered a conservation problem in the National Parks of this region (Lanin, Nahuel Huapi, Lago Puelo and Los Alerces) (Fernández, 2007), and since 2021 is listed as a major “Invasive Alien Species” in Argentina (Boletín Oficial de la República Argentina, 2021). The spread of *C. scoparius* can generate diverse impacts like limiting grazing, the access to recreation facilities, and timber production (Prasad, 2000). Outside its natural range it has no natural parasites or predators to limit its spread (Prasad, 2002). *C. scoparius* is also adaptable to varying ecological conditions and can grow on dry and poor soils, outcompeting other vegetation due to its nitrogen-fixing ability (Hosking et al. 1996; Prasad, 2000; Zouhar, 2005). Once established, it is extremely difficult to control because of its high seed production (Smith & Harlen,1991) and its capacity to regrow from any remaining shoots after cutting (Dougherty & Reichard, 2004). Another possible impact of *C. scoparius* could be to increase the fire hazard. Although it does not show highly flammable leaf characteristics (Blackhall et al. 2019), the concentration of biomass in dense patches could be dangerous in the event of ignition (Van Wilgen & Richardson, 1985; Brooks et al. 2004). Thus, mapping the distribution of invasive *C. scoparius* population is important not only for conservation purposes but also for fire management strategies.

2.3. Classification model

2.3.1. Satellite imagery and mosaic construction

We assembled annual Sentinel-2 mosaics for the period 2017–2025 within the Google Earth Engine (GEE) platform (Gorelick et al. 2017), using the harmonized top-of-atmosphere reflectance collection (Level-1C; COPERNICUS/S2_HARMONIZED). Sentinel-2 is suitable for this study given its 10 m spatial resolution and high revisit frequency, which enable the derivation of phenological metrics that improve land cover classification accuracy (Phiri et al. 2020). Scenes with more than 40 % cloud cover

pixels were discarded, and the remaining observations were further masked with the Cloud Score+ product (Pasquarella et al. 2023) using a clear-sky probability threshold of 0.6. Each annual mosaic was assembled from two complementary seasonal composites designed to capture the phenology of *C. scoparius.* First, a late-spring composite (November–December of year t), generated by retaining, for each pixel, all bands from the date of maximum Normalized Difference Yellowness Index, calculated with the multi-spectral blue (B2) and green (B3) bands (NDYI = (B3 − B2) / (B3 + B2); Sulik & Long, 2016), which emphasizes the conspicuous yellow flowering of the species. Second, a late-summer composite (February of year t + 1), generated as the per-pixel median of the visible and near-infrared bands. The two composites were stacked into single ten-band feature stack containing the blue (B2), green (B3), red (B4) an the near-infrared (B8) reflectances together with NDYI for each season, all at the native 10 m resolution. Permanent water, identified with a normalized difference water index computed from the green and near-infrared bands ((B3 − B8) / (B3 + B8) ≥ 0) and pixels above 1100 m a.s.l. (SRTM; Farr et al. 2007) were masked, restricting the analysis to the elevation range considered suitable for *C. scoparius* establishment in the study area, based on its invasion of similar temperate mountain ecosystems, such as those of New Zealand (Williams, 1981;Thomas et al. 2025). After masking, the classified area amounted to 950,119 ha, 38 % of the study-area polygon. Every classification and accuracy figure reported below refers to that classified area.

2.3.2. Reference data and first-stage Random Forest (RF1)

Reference polygons were digitized manually in Google Earth Pro on very-high-resolution imagery acquired during the November–December flowering period. Prior field knowledge of established *C. scoparius* patches was used as a spatial guide for locating candidate sites, but every polygon was re-delineated against the Earth Pro imagery, so that boundaries reflected the actual extent of flowering individuals rather than the approximate field outline. Because polygon digitization depended on the availability of cloud-free flowering-period scenes, the temporal coverage of the *C. scoparius* polygons was restricted to those years for which suitable Earth Pro imagery existed. For each year, between 10 to 15 polygons were digitized around clear flowering aggregations (visible bright-yellow canopy signals), and, 13 to 40 polygons over non-invaded native vegetation patches to serve as negative controls, adding up to 87 *C. scoparius* polygons (72.3 ha in total; median 0.32 ha, range 0.03–8.5 ha) and 150 control polygons (2,047 ha in total; median 3.9 ha, range 0.03–140 ha) across the seven years with suitable flowering-period imagery (2017–2023). Invasion polygons were manually digitized over large, homogeneous, and pure patches that exhibited a clear and unambiguous spectral signal, while control polygons were made to encompass all possible heterogeneity of the study area. A first Random Forest classifier (RF1; Breiman, 2001) was then trained, in GEE, to discriminate *C. scoparius* from background vegetation on each annual Sentinel-2 mosaic. Training samples were obtained by stratified random sampling within the reference polygons to account for the large differences in area between the two classes: all pixels from inside *C. scoparius* polygons (n=9,651) and 15,000 random points inside control polygons. *C. scoparius* samples were extracted exclusively from the year of digitization of their source polygon, whereas control samples were drawn across all years to capture the spectral variability of the

background, so that RF1 was fitted on 9,651 *C. scoparius* and 135,000 control observations. RF1 was implemented with the Statistical Machine Intelligence and Learning Engine learner (smileRandomForest; Li, 2014) using 500 trees and the ten spectral and index features described above. Each annual RF1 prediction was then post-processed with a connectivity filter that reclassified as background every *C. scoparius* pixel belonging to a patch of fewer than 5 contiguous pixels, with patch extent evaluated up to a search limit of 50 pixels, removing isolated commission errors generated by spectrally similar background units. The classifier was finally refined in a single iteration: visual inspection of the temporally consistent samples derived from its predictions (Section 2.3.3) revealed background units that were being systematically misclassified as *C. scoparius*, so additional control polygons were digitized over those units, added to the reference set, and the RF1 classifier was re-trained.

2.3.3. Stable-sample definition

The reference polygons described above inherit two limitations from the way they were generated: a temporal bias, because they cover only those years for which flowering-period high-resolution imagery was available in Google Earth Pro, and a spatial bias, because they coincide with the subset of *C. scoparius* patches that were known from previous field surveys. To mitigate both effects, we exploited the temporal coherence of the filtered RF1 series to derive an enlarged, internally consistent training pool spanning the full temporal and spatial extent of the annual Sentinel-2 mosaics. The nine annual filtered RF1 predictions were stacked, and for each pixel, the number of years in which it had been classified as *C. scoparius* was computed. From this stack we defined four temporal-stability classes as follows: stable *C. scoparius* (classified as *C. scoparius* in all 9 years), quasi-stable *C. scoparius* (8 of 9 years), stable background (never classified as *C. scoparius*) and quasi-stable background (classified as *C. scoparius* in only 1 of 9 years). All remaining pixels, whose label fluctuated more strongly across years, were discarded as ambiguous and were not used for the downstream classification. This rule sets apart pixels whose multi-annual behavior is internally consistent and therefore unlikely to reflect spurious classification noise, while propagating reliable labels to years and locations that were not represented in the original photo-interpreted polygon set.

2.3.4. Second-stage Random Forest (RF2)

A second Random Forest (RF2) was trained on the stable samples to refine the *C. scoparius* map. A single stratified sample of 40,000 pixel locations was drawn from the four stability classes (8,000 from each of the two *C. scoparius* classes and 12,000 from each of the two background classes), and the four-class label was collapsed into the original binary target by merging the stable and quasi-stable variants of each class. The spectral features of the 40,000 training locations were then extracted from each of the nine annual mosaics, yielding approximately 360,000 training observations. Because the same locations are revisited every year, these observations are nine temporal replicates of the same sites rather than spatially independent samples. RF2 was trained on the pooled multi-year sample with the

same ten-feature stack and the same hyperparameters as RF1 (500 trees, smileRandomForest), yielding a single, temporally generalized classifier that was subsequently applied to every annual mosaic.

2.3.5. Post-classification filtering of RF2

Two sequential filters were applied to the annual RF2 predictions. First, we filled temporal gaps by enforcing multi-year consistency: pixels classified as *C. scoparius* in 8 of the 9 years were assigned to *C. scoparius* in the remaining year, and pixels classified as background in 8 of the 9 years were assigned to background in the remaining year. This step removes isolated single-year anomalies driven by residual cloud contamination or phenological outliers; because the rule is evaluated on the whole series at once, the pixels it affects become constant across the nine years by construction. Second, we applied a connectivity filter, similar to the one used for RF1, that reclassified as background every *C. scoparius* patch of fewer than 3 contiguous pixels, with patch extent evaluated up to a search limit of 50 pixels, to remove residual isolated misclassifications. The resulting binary map for each year, at 10 m resolution, constitutes the final *C. scoparius* map for further analysis.

2.3.6. Validation

Map accuracy was assessed against an independent reference dataset built by blind photo-interpretation, following the good practices of Olofsson et al. (2014). Validation points were allocated by stratified random sampling of the final map itself, using three strata that partition the classified area: pixels mapped as *C. scoparius* in 2017 and/or 2025 (S1; 1,244 ha, 0.13 % of the classified area), background pixels within 1 km of mapped *C. scoparius* (S2; 70,344 ha, 7.4 %), and the remaining background (S3; 878,530 ha, 92.5 %). The number of points per stratum was set with the sample size formula of Olofsson et al. (2014) for a target standard error of 0.02, giving 400, 400 and 119 points respectively (919 in total), with a minimum separation of 500 m between points of the same stratum. The first and the last year of the series (2017 and 2025) were validated with this same set of points.

Each point was interpreted on very-high-resolution imagery in Google Earth Pro, complemented by a purpose-built GEE application that displayed the raw Sentinel-2 mosaics and the NDYI and NDVI time series of the pixel; neither tool ever displayed the classification. Three interpreters took part; points in S1 were assigned to two of them and those in S2 and S3 to one, with all interpreters working blind to the classified map. Like the model that is being validated, the interpreters assigned each pixel to one of two possible labels: *C. scoparius* invasion or background. Every label was recorded together with a confidence score from 0 to 10: a point-year was discarded when no interpreter reached a confidence of 5, and disagreements in labeling within a pair were resolved in favor of the more confident interpreter when the odds ratio of their confidences exceeded 2, and discarded otherwise. Agreement within pairs in S1 was moderate (Cohen's $\kappa = 0.55$ in 2017 and 0.52 in 2025), reflecting some uncertainty in the delineation of the reference data, particularly for points near the boundaries of *C. scoparius* patches, where consistent interpretation is difficult at the spatial resolution of Sentinel-2. This measure

characterizes the reliability of the reference rather than the accuracy of the map. We report the confusion matrix of each validated year together with overall accuracy (OA), producer's and user's accuracy (PA and UA) and their complementary omission and commission errors (OE and CE) for both classes, with 95 % Wilson confidence intervals, which remain within [0, 1] and give an informative upper bound when a count is zero. Because the sample is stratified with a deliberately disproportionate allocation (400 points over 1,244 ha in S1 against 119 points over 878,530 ha in S3), these figures describe the sample as it was drawn, that is, the accuracy of the map within the sampled locations and their immediate surroundings, and are not unbiased estimators of accuracy over the whole classified area. Area-weighted estimator of overall accuracy (OA, Olofsson et al. 2014) was also computed restricted to S1 ∪ S2 set, because that union is the domain in which the classifier has to discriminate *C. scoparius* from a non-trivial background.

2.4. Occupation and spatial extent analysis

We first fitted a descriptive model using the final RF2 classification across all years and the entire study area. For this, we extracted the subarea categories -urbanization, roads, rivers, (Instituto Geográfico Nacional 2025) and National Parks (Administración de Parques Nacionales 2025)- from available public shapefiles. For roads and rivers, we delimited a buffer of 20 m wide from its center. We fitted the data with a Generalized Additive Model (GAM) with a normal distribution using the mgcv R package (Wood, 2017). The response variable was the annual area occupied by *C. scoparius,* calculated as the sum of all 75.14 m^2 pixels (EPSG:4326; based on Sentinel pixel shape over the study area) classified asinvaded in each year. We included the subarea type as a fixed effect, and fitted a subarea-specific smooth term for the year, allowing temporal trajectories to differ among subarea types. To avoid excessive temporal flexibility, the smooth terms were constrained using a basis dimension of $k = 3$.

In order to analyze *C. scoparius* invasion patterns in relation to different predictors, we defined a 1000 × 1000 m geographical grid covering the study area. For each cell on the grid, we calculated the area (ha) occupied by *C. scoparius* in each year, the area (ha) and percentage (%) of urban cover for all years available (up to 2024), the percentage of National Park area (%), and the accumulated length of roads, rivers and lake shorelines (m). The urban area layers by year were obtained from the MapBiomas Land Cover and Land Use Collection (MapBiomas Project, 2025). Because *C. scoparius* is often associated to disturbance, we also calculated the percentage of each grid cell affected by fires over the last 20 years using the map created by Barberá et al. (2023). We also incorporated the mean value for three environmental variables – mean monthly temperature (C°), mean monthly precipitation (mm), elevation (m)- calculated for each grid cell using Google Earth Engine (Gorelick et al. 2017).

Due to the spatial nature of the data, we fitted generalized linear models that explicitly incorporate the spatial dependence among nearby observations using the spmodel package in R (Dumelle et al. 2023). This package allowed us to specify different spatial covariance structure; we tested four alternatives in all models: gaussian, exponential, spherical and a model without spatial covariance. For

each response variable, we selected the one with lower AIC value as the best model. Subsequently, with the gstat R package (Gräler et al. 2016), we examined residual variograms to confirm that the selected model exhibited weaker spatial structure than those of the original data, indicating that the models successfully accounted for most of the spatial correlation. We also assessed the spatial correlation using Moran's I test implemented in the spdep R package (Bivand et al. 2022).

The occurrence of *C. scoparius* in the 1000 x 1000 m cells was fitted with a binomial (link = logit) with a spherical spatial structure. Three coverage variables (urban settlements, national parks, historic fires), three cumulative length variables (roads, rivers and lake shorelines) and three environmental variables (temperature, precipitation, elevation) of each cell were included as additive predictors without interaction terms. Two quadratic terms were added for urban settlement area and elevation. Since our study area was really large, and invasion events relatively rare, we retained all *C. scoparius* presence records but only a random representative subset of available absence cells (10 times the number of presences). Consequently, the predicted probabilities should not be interpreted as estimates of the true occurrence probability in the landscape. However, this sampling design does not affect the shape or direction of the relationships between predictor variables and occurrence (Wang, 2020).

The spatial extent of *C. scoparius* invasion was quantified as the percentage of pixels occupied within the 1000 x 1000 m cells (hereafter, coverage). This variable was fitted with a gamma (link = log) with an spherical spatial structure. Similarly to the previous model, three coverage variables (urban settlements, national parks, historic fires), three corridor variables as cumulative length (roads, rivers and lake shorelines) and three environmental variables (temperature, precipitation, elevation) of each cell were included as additive predictors, omitting interaction and quadratic terms. The data set for this model included all the cells with presence, so estimates can be interpreted as true probability of cover.

Lastly, we fitted a model for the change in cover of *C. scoparius* in the 1000 x 1000 m cells between the mean cover of the first three years of the study (2017-2018-2019) and the last three years that included urban change data (2022-2023-2024), with an exponential spatial structure. As predictor we used the average change in urban area between the same years as the response variable.

2.5. Management strategies

To assign management practices across the study area, we analyzed landscape invasion metrics and developed a management index following a workflow similar to that proposed by Buchholtz et al. (2023). Using the 1000 x 1000 m grid of the study area we calculated three area-based landscape metrics for each grid cell: (i) the number of invaded patches, (ii) the total invaded area, and (iii) the largest patch index, defined as the percentage of the grid cell occupied by the largest invaded patch. For each metric, values were classified into low, intermediate, and high categories using the 0.33 and 0.66 quantiles as thresholds. Based on these metrics, we developed a four-level management index following the terminology proposed by Robertson et al. (2020). Cells with no invaded patches were classified as *No invasion,* where no management is required. Invaded cells were classified as *Eradication* when at least

two of the three metrics fell within the lower quantile range, indicating small and localized invasions where it exists the possibility to permanently remove every *C. scoparius* patch, with no immediate risk of re-invasion. Cells were classified as *Containment* when at least two metrics were within the upper quantile range, representing extensive and well-established invasions, where control measures might require excessive effort but measures to prevent spreading could be applied. All remaining invaded cells were classified as *Complete Reproductive Removal* (from now on *C. R. Removal*), corresponding to intermediate invasion scenarios where removal of reproductive population would be feasible but, due to patch extension, efforts and costs too high to eradicate seedlings, therefore there is high risk of re-invasion and further reproduction. Metrics were calculated with the landscapemetrics R-package (Hesselbarth et al. 2019).

All analyses were performed in R v4.6.0 (R Core Team, 2026). All data and code supporting this study are publicly available in a GitHub repository (*https://github.com/LicanMartinez/Retamap*).

3. Results

3.1. *C. scoparius* invasion maps and dynamics

The final Random Forest model predicted the recent spatial distribution of *C. scoparius* across the study area (Figure 1). For visualization, we made a map for the most recent year analyzed (2025, Figure 1), remaining years and supplementary spatial results can be accessed through *https://github.com/LicanMartinez/Retamap*. Overall, the independent validation supported the reliability of the final *C. scoparius* distribution maps, with high overall accuracy and high reliability of pixels classified as invaded, while indicating that remaining errors were primarily associated with omission of invaded pixels. The details of this validation can be seen at the next section.

The invasion of *C. scoparius* estimated for the whole study area was maximum in 2018 with a total of 1039 ha invaded. Thereafter, invaded area detected declined markedly, reaching a minimum of 618 ha in 2021. Then the invaded area increased gradually, peaking again at 812 ha in 2024, before decreasing to 726 ha in 2025. Overall, the fitted GAM indicated a decline in the invaded area during the first half of the study period followed by a moderate increase in recent years (Figure 2A). Temporal trends in the area occupied by *C. scoparius* differed slightly among landscape features (Figure 2B). Within National Parks, the invaded area remained relatively low and stable, with *C. scoparius* occupying [0.01-0.01]% of the subarea across the study period (National Park available for invasion = 62.46%). Urban settlements showed a marked decline, from [1.06]% to [0.70]%, followed by relatively stable values after 2020 (Urban settlements available for invasion = 1.72%). In contrast, areas outside National Parks and outside urban settlements, which encompassed the largest proportion of the study area available for invasion, contained the largest invaded area and exhibited more stable values following the same trend as the whole study area results. Similar temporal patterns were observed along roads and rivers, although the area occupied by *C. scoparius* within river buffers was substantially lower than in all other categories (Rivers buffer available for invasion 0.93% and roads buffer available for invasion 0.62%).

The probability of occurrence and cover in 1000 x 1000 m cells was modulated by different variables, with the strongest effects associated with corridor-related variables (Figure 3 & 4, Figure S1 & S2). Occurrence probability was markedly higher in areas with more road length and, to a lesser extent, with higher values of river and lakes shoreline length. Urban area showed a significant unimodal effect, with occurrence probability peaking at intermediate levels of urbanization and declining towards higher values. Mean elevation also exhibited a weak non-linear effect, with higher probabilities at lower and intermediate elevations (approx. 300–900 m a.s.l.). Mean monthly temperature was positively associated with occurrence probability, whereas mean monthly precipitation, National Park area, and fire-affected area showed no significant association with occurrence. Similar to the ocurrence, cover probability was positively associated with roads, rivers and lake shorelines length, specially with roads which increased the cover probability from 0.15 [IC: -0.07, +0.10] ha in cells without roads to 1.7 [IC: -0.95, +2.20] ha in cells containing 20 km of cumulative road length, representing approximately an increment of eleven times its invasion area. For rivers, cover probability increased from approximately 0.18 [IC: - 0.06, +0.11] to 0.55 [IC: -0.25, +0.50] ha across the observed gradient of cumulative river length (0–3.8 km), and from 0.17 [IC: -0.06, +0.11] to 0.60 [IC: -0.25, +0.50] ha across the gradient of cumulative lake shoreline length (0–3.6 km). Cover probability also increased with precipitation, rising from approximately 0.14 [IC: -0.04, +0.04] to 0.35 [IC:-0.14, +0.21] ha between 55 and 135 mm of mean monthly precipitation. Fire-affected area showed a weaker positive association, with cover probability increasing from about 0.20 [IC: -0.01, +0.01] to 0.31 [IC: -0.13, +0.21] ha between 0 and 100% of burned area. Urban settlement area, National Park area, mean monthly temperature and elevation showed no significant association over cover. Across the study area, the last model detected that change in *C. scoparius* cover was negatively associated with change in urban cover (Figure S3). For each 5 ha that urban cover increased, the area of *C. scoparius* wasreduced 0.15 ha [IC ± 0.075]. Because this trend was not homogeneous throughout the study area, the spatial distribution of positive and negative changes in *C. scoparius* cover between the first and last years analyzed were visualized in a map (Figure S4).

Based on landscape invasion metrics, management strategies were assigned to each cell (Figure 5). In total, 316 cells (1000 x 1000 m) were suitable for *Eradication* actions, 243 cells for *C. R. Removal*, and 310 for *Containment*. *Containment* cells were primarily concentrated in urban settlements, whereas *Eradication* and *C. R. Removal* cells were more common in urban-natural interfaces, and more heterogeneously dispersed throughout the rest of the study area. These cells contained 14 ha of invaded area classified for *Eradication*, 56 ha for *C. R. Removal*, and 656 ha for *Containment*.

3.2. Validation metrics

Independent validation of the final map returned an overall accuracy of 92.6 % in 2017 and 92.9 % in 2025 (Table 1a). Errors were markedly asymmetric: commission of the *C. scoparius* class stayed close to 9 % in both years, whereas omission was the dominant error and varied from 12.1 % to 16.0 %. None of the background stratum points distant from mapped *C. scoparius* (S3) turned out to be invaded (0 of 105 points in each year, with an upper 95 % bound of 3.5 %), indicating that the invasion missed by the map occurs in the surroundings of already mapped patches rather than scattered across the study area.

Restricted to that domain (S1 ∪ S2), where the classifier has to discriminate *C. scoparius* from non-trivial background, the area-weighted overall accuracy was 98.6 % [97.4–99.7] in 2017 and 98.0 % [96.6–99.4] in 2025. The higher User's Accuracy relative to Producer's Accuracy indicates that pixels classified as *C. scoparius* were reliable, although a non-negligible proportion of invaded pixels remained undetected (Table 1b).

4. Discussion

In this study, we mapped the distribution of invasive populations of *C. scoparius* in North Patagonia and identified variables associated with its occurrence and coverage, as well as the temporal dynamics of the invaded area. Our approach provides a level of spatial and temporal depth not achieved in earlier studies, with a high-resolution map of the invasion across a large geographical extent over a 9-year period. Fndings indicate that *C. scoparius* is concentrated inside urban settlements, where the highest densities of the species occur, and declines toward the urban–natural interface and natural areas. Temporal analysis showed that its total distribution had a decline followed by relative stability during the last years. However, this regional trend was spatially heterogeneous, as some areas gained cover while others lost it. While most subarea types broadly followed the regional pattern, with more areas experiencing losses in invasion cover, National Parks were the only landscape feature showing an apparent stable dynamic throughout the years analyzed. Our results suggest that urbanization not only represents a hotspot for invasion, but also urban expansion may be a major driver of the observed decrease of invasion cover over time. In addition, the invasion is associated with both anthropogenic and natural dispersal corridors, mainly roads. Additionally, we developed spatially explicit management strategies recommendations across the study area, presenting a practical tool for prioritizing management actions and supporting decision-making processes.

The relation of invasive population occurrence and cover with the tested predictors shared a common pattern: a strong effect of anthropogenic corridors, followed by a weaker effect of natural dispersal corridors. Corridors, both anthropogenic and natural, facilitate propagule transport while their recurrent disturbance creates favorable conditions for establishment, allowing connectivity among invasion patches. Like many invasive species (Aranda et al. 2024), *C. scoparius* takes advantage of disturbed environments. Our results are consistent with studies conducted both in its native range (Paynter et al. 2000) and in regions where the species present invasive populations (Rees & Paynter 1997). Roads, for example, experience constant earth movement along their sides, either for maintenance or new infrastructure, and seed dispersal may also be facilitated by vehicles (Von der Lippe & Koarik 2006). On the other hand, rivers and lake shorelines are affected by seasonal changes in water flow or water level which also generate constant disturbance. These disturbances create open environments generating optimal conditions, which, added to the ballistic seed ejection mechanism of the species, makes these linear corridors optimal for establishing and spreading (Anđelković & Radulović 2022). Beyond the effect of corridors, topographic, climatic, and disturbance factors were also associated with population occurrence and coverage, although their effects differed between them.

The association of occurrence with low to intermediate elevations (approx. 300–900 m a.s.l.) and higher mean temperatures suggests that current climatic suitability constrains the broad distribution of the species, although this constraint may shift under climate change (Barros et al. 2025). In contrast, once established, *C. scoparius* cover is associated with more precipitation and a larger proportion of fire-affected areas, suggesting that water availability facilitates patch expansion and biomass accumulation (Montero-Castaño et al. 2023), and fire enhances spread by creating favorable post-disturbance conditions (Huerta et al. 2022; Paynter et al. 1998). Given that *C. scoparius* is already present along most of the main roads and that it thrives in disturbed environments, projected increases in fire frequency and extent (Kitzberger et al. 2022) may create new opportunities for expansion into new ecosystems. This risk may be further enhanced because most ignitions are associated with human infrastructure, making this process particularly important along anthropogenic corridors.

Urbanization also showed an important role in the invasion process, particularly over the species occurrence. The observed pattern, in which the highest probability of ocurrence of *C. scoparius* occurs at intermediate levels of urban settlement cover and declines when urban cover is either low or high, is similar to patterns reported for non-native plants along urbanization gradients. Intermediate levels of urbanization potentially combines high propagule pressure with greater habitat heterogeneity (Cubino et al. 2015; Montagnani et al. 2026). Intermediate levels of urbanization may act as important sources of propagules, reflecting the historical use of *C. scoparius* as an ornamental species (Rovere et al. 2013), while also facilitating population establishment through anthropogenic disturbance. However, at higher levels of urbanization, the amount of suitable habitat available for *C. scoparius* may decrease as urban infrastructure replaces invaded patches. This is consistent with the idea that highly urbanized areas can impose stronger habitat constraints (Potgieter et al. 2024). This spatial pattern was also reflected in the temporal dynamics, as continued urban expansion was associated with declines in *C. scoparius* cover. While the greatest declines occurred where urban areas expanded the most, urbanization should not be considered to have a positive impact over the ecosystem, nor should it be viewed as way to control the invasion. Urban expansion may replace both invaded and non-invaded area, homogenizing the landscape (McKinney 2006) and reducing available habitat for native species, while simultaneously being a foci for the spread of invasive individuals. In this sense, although the mechanism is different, both urbanization and biological invasion contribute to biotic homogenization by reducing the available habitat for natives and favoring a limited set of species, mainly invasive species tolerant to disturbance and prefered by urban settlers (McKinney 2006, Zuñiga-Palacios 2026).

Temporal dynamics also revealed spatial heterogeneity in *C. scoparius* cover. The observed pattern of invasion cover decrease in some areas, whereas others showed local gains probably reflects the combined effects of management and local population spread. Populations may decline following control efforts but subsequently recover if management is not sustained, while populations in other areas may spread or become detectable as they increase in size. National Parks were the only subarea type wihere apparent stability was observed, which resulted from compensatory gains and losses of invasion cover areas. Apparent cover losses following management may not always represent a real reduction in population size, but rather a failure of detectability. This could be the case for the overall

cover decrease in urban settlements and along roads. Roadside management is commonly based on single control events, after which individuals can resprout. Because *C. scoparius* may require at least three years to regain sufficient size and reproductive capacity to produce the flowering signal used for detection (Parker, 1997; Peterson & Prasad 1998; Sheppard et al. 2002), recently managed populations could remain undetected by the classification model. Nevertheless, given the long temporal coverage of our analysis, temporary reductions in detectability are unlikely to account for the overall temporal patterns observed.

Invasive species populations often occupy a relatively small proportion of the landscape, yet their ecological and socioeconomic impacts can be large (Bradley et al. 2019). Even localized invasions can alter ecosystem processes, affect native biodiversity, and act as sources for further spread across the landscape (Bradley et al. 2019). *C. scoparius* invasive populations currently cover 726 ha across the study area, highlighting that even a spatially limited invasion can represent a substantial management challenge. Furthermore, areas with similar invaded area may require different management actions depending on how the invasion is spatially configured (Eppinga et al 2021). The proposed management strategies we presented, based on invasion cover and landscape configuration for each invaded area aligns within a framework that recognizes that different invasion stages and configurations require different management objectives (Robertson et al. 2020). The high percentage of the invaded area suited for management actions focused on limiting further spread rather than complete or partial removal (*Containment* 90,4%; *C. R. Removal*7.7%; *Eradication* 1.9%), indicates that the invasion has reached a stage where opportunities for removal are relatively limited across the study area. This may involve greater effort and resources, as containment requires sustained management to be effective. In addition, the heterogeneous distribution and large spatial extent of the management strategies represents a logistical challenge, as interventions would need to be distributed across multiple and spatially separated locations. This situation makes clear the importance of prioritizing areas before applying management actions. As invasive individuals grow and invaded area increases, management costs are expected to rise while control efficiency declines (Moyano et al. 2025), highlighting the benefits of early intervention. Together with the experience of park agents and other possible interested actors (NGOs, researchers, etc), our study can be used to assign priority areas and support management planning. Final prioritization should also consider local conservation priorities, including areas of high biodiversity value, public use areas, accessibility, available resources, and other priorities identified by park agents (Ziller et al, 2020; Courtois et al. 2023; Carter et al 2024) Moreover, this tool could be adapted to other species of interest. Because plant communities are usually invaded by multiple invasive species, the development of an integrative prioritization scheme that considers the distribution of invasive communities rather than individual species could enhance resource allocation and management efficiency. In this context, our approach provides a solid base for developing such a framework in the future.

While the map proved to be accurate within the invaded areas and their surroundings, some limitations should be considered. First, image availability varied among years because the study area is located in a temperate region with frequent cloud cover, even during the dry season used for image

selection. Also, large forest fires occurring during this season generated smoke plumes that likely reduced image quality and surface visibility in some areas and years (Shi et al. 2024; Barberá et al. 2023). Similar to other studies that rely in phenology (Bradley 2014), interannual variation in *C. scoparius* flowering phenology may have shifted the timing and duration of the spectral signal used for classification, potentially affecting detectability among years. Finally, although *C. scoparius* predominantly invades open environments, individuals growing under open forest canopies may have remained undetected because their spectral signal was obstructed. This is consistent with our validation, in which omission was the dominant error and was concentrated around the mapped patches, where the invasion is sparser and more recent. These challenges are inherent to satellite detection of invasive species and are not unique to our study; similar limitations have been reported in remote sensing studies of invasive pines in Patagonia, where dispersed invasion fronts were more difficult to detect than dense stands (Bagnato et al. 2025). Nevertheless, because the invasion that escaped detection was confined to the surroundings of the patches already mapped, these limitations are more likely to affect the absolute extent of the invasion than the broad spatial and temporal patterns identified in our study.

The approach we have used here is low-cost, effective, and potentially transferable. Our study adds to the growing evidence that species phenology can be used to detect invasive plants using satellite imagery by extending this approach to a large geographical extent and a long temporal series, while demonstrating its direct application to management planning. More broadly, our results demonstrate the value of high-resolution satellite imagery as a tool for long-term invasion monitoring. This approach will facilitate the continuous assessment of species establishment, expansion, decline, and responses to management, supporting adaptive management over time.

Declarations

Acknowledgments

The authors would like to acknowledge Juan H. Gowda and Romina González Musso which encouraged us to carry on this project, and for the help they provided at the initial stage. We are also grateful for the guidance and intellectual input provided by Camilo E. Bagnato in regards of validation of our model. Finally, we would like to thank Gloria Fernández Canepa and Carla M. Pozzi for clarifying us questions regarding the *C. scoparius* invasion in Nahuel Huapi National Park.

Funding

This work was mainly funded by a “Rufford small grants” (44748-1) from The Rufford Foundation awarded to Sofía Cingolani.

Competing interests

The authors declare no conflict of interest.

Author information

Authors and Affiliations

Grupo de Investigaciones en Biología de la Conservación, INIBIOMA, Universidad Nacional del Comahue-CONICET, Bariloche, Río Negro, 8400, Argentina

Sofía Cingolani & Karina L. Speziale
Grupo de Ecología de la Polinización, INIBIOMA, Universidad Nacional del Comahue-CONICET, Bariloche, Río Negro, 8400, Argentina

Licán E. Martinez

Grupo de Ecología de Invasiones, INIBIOMA, CONICET, Universidad Nacional del Comahue, San Carlos de Bariloche, Argentina

Jaime Moyano

Corresponding author

Correspondence to Sofía Cingolani .

Contributions

All authors contributed to the study conception and design. Material preparation, data collection and analysis were performed by Sofía Cingolani and Licán E. Martinez. The first draft of the manuscript was written by Sofía Cingolani with contributions from Licán E. Martinez in the methodology section. All authors commented on previous versions of the manuscript. All authors read and approved the final manuscript.

References

1. Administración de Parques Nacionales. (2007, 24 de julio). Resolución N.º 172/2007. Lineamientos estratégicos para el manejo de especies exóticas. Sistema de Información de Biodiversidad. sib.gob.ar
2. Anđelković, A., & Radulović, S. (2022). The role of riparian areas in alien plant invasions. Acta herbologica, 31(2), 93-104. *DOI*:10.5937/actaherb2202093A

3. Aranda, M. J., Conedera, M., Pezzatti, G. B., & Gehring, E. (2024). Landscape, site and post-disturbance forest stand characteristics modulate the colonisation of non-native invasive woody species. Forest Ecology and Management, 565, 122017.
4. Barberá, I., Paritsis, J., Ammassari, L., Morales, J. M., & Kitzberger, T. (2023). Microclimate and species composition shape the contribution of fuel moisture to positive fire-vegetation feedbacks. *Agricultural and Forest Meteorology*, *330*, 109289.
5. Barros, A., Fuentes Lillo, E., Aschero, V., Pauchard, A., Alvarez, M. A., Wedegärtner, R., ... & Lembrechts, J. J. (2025). Beyond the Trail—Understanding Non-Native Plant Invasions in Mountain Ecosystems. Global Ecology and Biogeography, 34(6), e70060.
6. Blackhall, Melisa, and Estela Raffaele. "Flammability of Patagonian invaders and natives: When exotic plant species affect live fine fuel ignitability in wildland-urban interfaces." Landscape and urban planning 189 (2019): 1-10.
7. Brooks, M. L., D'antonio, C. M., Richardson, D. M., Grace, J. B., Keeley, J. E., DiTomaso, J. M., ... & Pyke, D. (2004). Effects of invasive alien plants on fire regimes. BioScience, 54(7), 677-688.
8. Bolch, E. A., Santos, M. J., Ade, C., Khanna, S., Basinger, N. T., Reader, M. O., & Hestir, E. L. (2020). Remote detection of invasive alien species. In Remote sensing of plant biodiversity (pp. 267-307). Springer, Cham.
9. Boyle, S.A.; Kennedy, C.M.; Torres, J.; Colman, K.; Pérez-Estigarribia, P.E.; De La Sancha, N.U. High-resolution satellite imagery is an important yet underutilized resource in conservation biology. PLoS ONE 2014, 9, e86908.
10. Bradley, B. A. (2014). Remote detection of invasive plants: a review of spectral, textural and phenological approaches. Biological invasions, 16(7), 1411-1425.
11. Bradley, B. A., Allen, J. M., O'Neill, M. W., Wallace, R. D., Bargeron, C. T., Richburg, J. A., & Stinson, K. (2018). Invasive species risk assessments need more consistent spatial abundance data. Ecosphere, 9(7), e02302.
12. Bradley B. A., Laginhas BB, Whitlock R, et al. (2019) Disentangling the abundance–impact relationship for invasive species. PNAS 116:9919–9924. https://doi.org/10.1073/pnas.1818081116
13. Breiman, L. (2001). Random forests. Machine Learning, 45(1), 5–32. https://doi.org/10.1023/A:1010933404324
14. Brooks, M. L., D'antonio, C. M., Richardson, D. M., Grace, J. B., Keeley, J. E., DiTomaso, J. M., ... & Pyke, D. (2004). Effects of invasive alien plants on fire regimes. BioScience, 54(7), 677-688.
15. Carrión-Klier, C.; Moity, N.; Sevilla, C.; Rueda, D.; Jäger, H. The Importance of Very-High-Resolution Imagery to Map Invasive Plant Species: Evidence from Galapagos. Land 2022, 11, 2026. https://doi.org/10.3390/land11112026
16. Carter, S., Mills, C., Hao, Z., Mott, R., Hauser, C.E., White, M., Sharples, J., Taylor, J. and Moore, J.L., (2024). Spatial prioritization for widespread invasive species control: Trade-offs between current impact and future spread. *Ecological Applications*, *34*(5), p.e2982.

17. Cavallero, L., Morales, C. L., Montero-Castaño, A., Gowda, J. H., & Aizen, M. A. (2018). Scale-dependent effects of conspecific flower availability on pollination quantity and quality in an invasive shrub. *Oecologia*, *188*(2), 501-513.
18. Courtois, P., Martinez, C., & Thomas, A. (2023). Spatial priorities for invasive alien species control in protected areas. *Science of the Total Environment*, *878*, 162675.
19. Cubino JP, Subirós JV, Lozano CB. 2015. Propagule pressure from invasive plant species in gardens in low-density suburban areas of the Costa Brava (Spain). . Urban For. Urban Green. 14:(4):941–51
20. Davis, M. A., Grime, J. P., & Thompson, K. (2000). Fluctuating resources in plant communities: a general theory of invasibility. Journal of ecology, 88(3), 528-534.
21. Dougherty, D., & Reichard, S. H. (2004). Factors affecting the control of Cytisus scoparius and restoration of invaded sites. Plant Protection Quarterly, 19(4), 137-142.
22. Eppinga, M. B., Baudena, M., Haber, E. A., Rietkerk, M., Wassen, M. J., & Santos, M. J. (2021). Spatially explicit removal strategies increase the efficiency of invasive plant species control. *Ecological Applications*, *31*(3), e02257.
23. Farr, T. G., Rosen, P. A., Caro, E., Crippen, R., Duren, R., Hensley, S., Kobrick, M., Paller, M., Rodriguez, E., Roth, L., Seal, D., Shaffer, S., Shimada, J., Umland, J., Werner, M., Oskin, M., Burbank, D., & Alsdorf, D. (2007). The Shuttle Radar Topography Mission. Reviews of Geophysics, 45(2), RG2004. https://doi.org/10.1029/2005RG000183
24. Franklin, S.E. (2010). Remote Sensing for Biodiversity and Wildlife Management; McGraw-Hill: New York, NY, USA.
25. Gorelick, N., Hancher, M., Dixon, M., Ilyushchenko, S., Thau, D., & Moore, R. (2017). Google Earth Engine: Planetary-scale geospatial analysis for everyone. Remote Sensing of Environment, 202, 18–27. https://doi.org/10.1016/j.rse.2017.06.031
26. Haubrock, P. J., Tarkan, A. S., Martín-Forés, I., Katsanevakis, S., Sousa, R., Soto, I., ... &
27. Britton, J. R. (2026). The spread of non-native species. Biological Reviews, 101(3), 1197-1234.
28. Hill, D. A., Prasad, R., & Leckie, D. G. (2016). Mapping of scotch broom (Cytisus scoparius) with landsat imagery. *Weed Technology*, *30*(2), 539-558.
29. Hobbs, H. A. M. R. J. (2000). *Invasive species in a changing world*. Island press.
30. Hosking, J. R., Sheppard, A. W., & Sagliocco, J. L. (2012). Cytisus scoparius (L.) Link–broom, Scotch broom or English broom.
31. Huerta, S., Marcos, E., Fernández-García, V., & Calvo, L. (2022). Resilience of Mediterranean communities to fire depends on burn severity and type of ecosystem. Fire Ecology, 18(1), 28.
32. IPBES. (2019). *Global assessment report on biodiversity and ecosystem services of the Intergovernmental Science-Policy Platform on Biodiversity and Ecosystem Services*. E. S. Brondízio, J. Settele, S. Díaz, and H. T. Ngo (Eds.). IPBES Secretariat, Bonn, Germany. https://doi.org/10.5281/zenodo.3831673

33. Kitzberger T, Tiribelli F, Barberá I, et al (2022) Projections of fire probability and ecosystem vulnerability under 21st century climate across a trans-Andean productivity gradient in Patagonia. Science of The Total Environment 839:156303. https://doi.org/10.1016/j.scitotenv.2022.156303
34. Lamb, D. W., & Brown, R. B. (2001). PA—Precision Agriculture. Journal of Agricultural Engineering Research, 78(2), 117–125. doi:10.1006/jaer.2000.0630
35. Li, H. (2014). Smile: Statistical Machine Intelligence and Learning Engine. Recuperado de https://haifengl.github.io
36. MapBiomas Argentina Project. (2025). *Collection 2 of the Annual Land Use and Land Cover Maps of Argentina*. Accessed 8 August 2026 at https://plataforma.argentina.mapbiomas.org/.
37. McKinney, M. L. (2006). Urbanization as a major cause of biotic homogenization. Biological conservation, 127(3), 247-260.
38. Meyer, S. E., Callaham Jr, M. A., Stewart, J. E., & Warren, S. D. (2021). Invasive species response to natural and anthropogenic disturbance. In Invasive species in forests and rangelands of the United States: A comprehensive science synthesis for the United States forest sector (pp. 85-110). Cham: Springer International Publishing.
39. Montagnani, C., Sebesta, N., Vegini, E. et al. Invasive alien plants and the city: distribution patterns in response to urban elements and urbanization in three of the largest cities in Italy. Urban Ecosyst 29, 14 (2026). https://doi.org/10.1007/s11252-025-01876-3
40. Montero-Castaño, A., Aizen, M. A., González-Moreno, P., Cavallero, L., Vilà, M., & Morales, C. L. (2023). Influential factors and barriers change along the invasion continuum of an alien plant. *Biological Invasions*, *25*(9), 2977-2991.
41. O'Neill, M. W., Bradley, B. A., & Allen, J. M. (2021). Hotspots of invasive plant abundance are geographically distinct from hotspots of establishment. Biological Invasions, 23(4), 1249-1261.
42. Olofsson, P., Foody, G. M., Herold, M., Stehman, S. V., Woodcock, C. E., & Wulder, M. A. (2014). Good practices for estimating area and assessing accuracy of land change. Remote sensing of Environment, 148, 42-57.
43. Parker, I. M. (1997). Pollinator limitation of Cytisus scoparius (Scotch broom), an invasive exotic shrub. Ecology, 78(5), 1457-1470.
44. Parker, I. M. (2000). Invasion dynamics of Cytisus scoparius: a matrix model approach. Ecological Applications, 10(3), 726-743.
45. Pasquarella, V. J., Brown, C. F., Czerwinski, W., & Rucklidge, W. J. (2023). Comprehensive quality assessment of optical satellite imagery using weakly supervised video learning. In Proceedings of the IEEE/CVF Conference on Computer Vision and Pattern Recognition Workshops (CVPRW) (pp. 2125–2135). https://doi.org/10.1109/CVPRW59228.2023.00206
46. Paynter, Q., Fowler, S. V., Memmott, J., & Sheppard, A. W. (1998). Factors affecting the establishment of Cytisus scoparius in southern France: implications for managing both native and exotic populations. Journal of Applied Ecology, 582-595.

47. Peterson, D. J., & Prasad, R. (1998). The biology of Canadian weeds. 109. Cytisus scoparius (L.) Link. Canadian journal of plant science, 78(3), 497-504.
48. Phiri, D.; Simwanda, M.; Salekin, S.; Nyirenda, V.R.; Murayama, Y.; Ranagalage, M. Sentinel-2 data for land cover/use mapping: A review. Remote Sens. 2020, 12, 2291. [CrossRef]
49. Potgieter, L. J., Li, D., Baiser, B., 0Kühn, I., Aronson, M. F., 0Carboni, M., ... & Cadotte, M. W. 0(2024). Cities shape the diversity 0and spread of nonnative species. 0Annual review of ecology, 0evolution, and systematics, 055(1), 157-180.
50. Rovere, A. E., Molares, S., & Ladio, A. H. (2013). Plantas utilizadas en cercos vivos de ciudades patagónicas: aportes de la etnobotánica para la conservación. Ecología austral, 23(3), 165-173.
51. Sheppard, A. W., Hodge, P., Paynter, Q., & Rees, M. (2002). Factors affecting invasion and persistence of broom Cytisus scoparius in Australia. *Journal of Applied Ecology*, 721-734.
52. Shi, Y. R., Levy, R. C., Remer, L. A., Mattoo, S., & Arnold, G. T. (2024). Investigating the Spatial and Temporal Limitations for Remote Sensing of Wildfire Smoke Using Satellite and Airborne Imagers During FIREX-AQ. Journal of Geophysical Research: Atmospheres, 129(2), e2023JD039085.
53. Smith, J. M. B., & Harlen, R. L. (1991). Preliminary observations on the seed dynamics of broom (Cytisus scoparius) at Barrington Tops, New South Wales.
54. Stout, J. C. (2000). Does size matter? Bumblebee behaviour and the pollination of Cytisus scoparius L.(Fabaceae). *Apidologie*, *31*(1), 129-139.
55. Sulik, J. J., & Long, D. S. (2016). Spectral considerations for modeling yield of canola. Remote Sensing of Environment, 184, 161–174. https://doi.org/10.1016/j.rse.2016.06.016
56. Thomas, P. A., Dering, M., Iszkuło, G., Kujawska, M., Łukowski, A., Rabska, M., ... & Giertych, M. J. (2025). Biological Flora of Britain and Ireland: Cytisus scoparius* No. 307. Journal of Ecology, 113(7), 1877-1933.
57. Trueman, M., Standish, R. J., & Hobbs, R. J. (2014). Identifying management options for modified vegetation: Application of the novel ecosystems framework to a case study in the Galapagos Islands. *Biological Conservation*, *172*, 37-48.
58. Van Wilgen, B. W., & Richardson, D. M. (1985). The effects of alien shrub invasions on vegetation structure and fire behaviour in South African fynbos shrublands: a simulation study. Journal of applied Ecology, 955-966.
59. Von der Lippe, M., & Kowarik, I. (2007). Long-distance dispersal of plants by vehicles as a driver of plant invasions. *Conservation Biology*, *21*(4), 986-996. https://doi.org/10.1111/j.1523-1739.2007.00722.x
60. Walsh, S. J. (2018). Multi-scale remote sensing of introduced and invasive species: An overview of approaches and perspectives. Understanding invasive species in the Galapagos Islands: From the molecular to the landscape, 143-154.
61. Wang, H. (2020, November). Logistic regression for massive data with rare events. In International conference on machine learning (pp. 9829-9836). PMLR.

62. Williams, P. A. (1981). Aspects of the ecology of broom (Cytisus scoparius) in Canterbury, New Zealand. New Zealand Journal of Botany, 19(1), 31–43. https://doi.org/10.1080/0028825X.1981.10425187
63. Ziller, S. R., de Sá Dechoum, M., Silveira, R. A. D., da Rosa, H. M., Motta, M. S., da Silva, L. F., ... & Zenni, R. D. (2020). A priority-setting scheme for the management of invasive non-native species in protected areas. *NeoBiota*, *62*, 591-606.
64. Zouhar, K. (2005). Cytisus spp.: Cytisus scoparius, C. striatus, brooms: Scotch broom, striated broom. *Fire Effects Information System,[Online]. US Department of Agriculture, Forest Service, Rocky Mountain Research Station, Fire Sciences Laboratory (Producer). Available: https://research. fs. usda. gov/feis/species-reviews/cytspp*.
65. Zuñiga-Palacios, J., I. Zuria, and C. E. Moreno. 2026. Global Patterns and Drivers of Urban Biotic Homogenization: A Meta-Analysis. *Global Ecology and Biogeography* 35, no. 3: e70219. https://doi.org/10.1111/geb.70219.

Tables

Table 1. Results of the independent validation of the final map, for the first and the last year of the series. Values are percentages, with their 95 % Wilson confidence interval in brackets, computed on the validation sample (Section 2.3.6). a. Overall accuracy, and producer's and user's accuracy with their complementary omission and commission errors, for the *C. scoparius* and the background classes; the last rows give the area-weighted overall accuracy restricted to the mapped patches and their surroundings (S1 ∪ S2) and the number of validated point-years. b. Confusion matrix, as counts of validated point-years (TP, true positives; FP, false positives; FN, false negatives; TN, true negatives).

a.

Metric	2017	2025
Overall accuracy	92.6 [90.6–94.2]	92.9 [90.9–94.4]
User's accuracy, *C. scoparius*	90.2 [86.1–93.2]	90.9 [86.3–94.0]
Producer's accuracy, *C. scoparius*	87.9 [83.6–91.2]	84.0 [78.8–88.1]
Commission error, *C. scoparius*	9.8 [6.8–13.9]	9.1 [6.0–13.7]
Omission error, *C. scoparius*	12.1 [8.8–16.4]	16.0 [11.9–21.2]
User's accuracy, background	93.8 [91.5–95.6]	93.6 [91.3–95.3]
Producer's accuracy, background	95.0 [92.9–96.6]	96.5 [94.7–97.7]
Overall accuracy within S1 ∪ S2 (area-weighted)	98.6 [97.4–99.7]	98.0 [96.6–99.4]
Validated point-years (n)	826	813

b.

Predicted / Reference	*C. scoparius* (2017)	Background (2017)	*C. scoparius* (2025)	Background (2025)
C. scoparius	248 (TP)	27 (FP)	199 (TP)	20 (FP)
Background	34 (FN)	517 (TN)	38 (FN)	556 (TN)

Figures

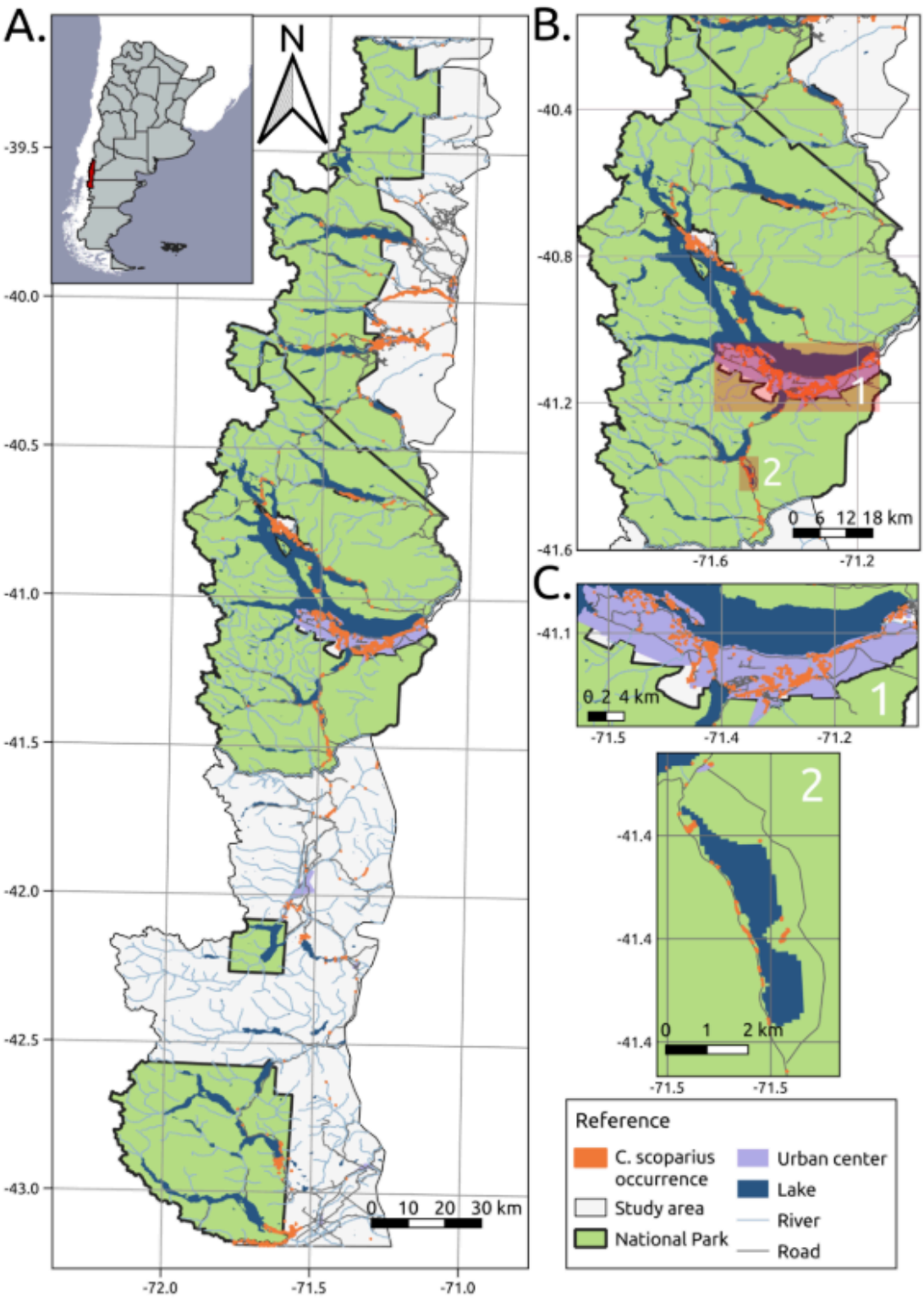


Figure 1

A. Cover of *C. scoparius*invasion in the study area for the most recent year sampled (2025). **B.**Detail of Nahuel Huapi National Park showing two subareas: **(1)** the urban area of San Carlos de Bariloche and **(2)** a non-urbanized area surrounding Lake Guillelmo.

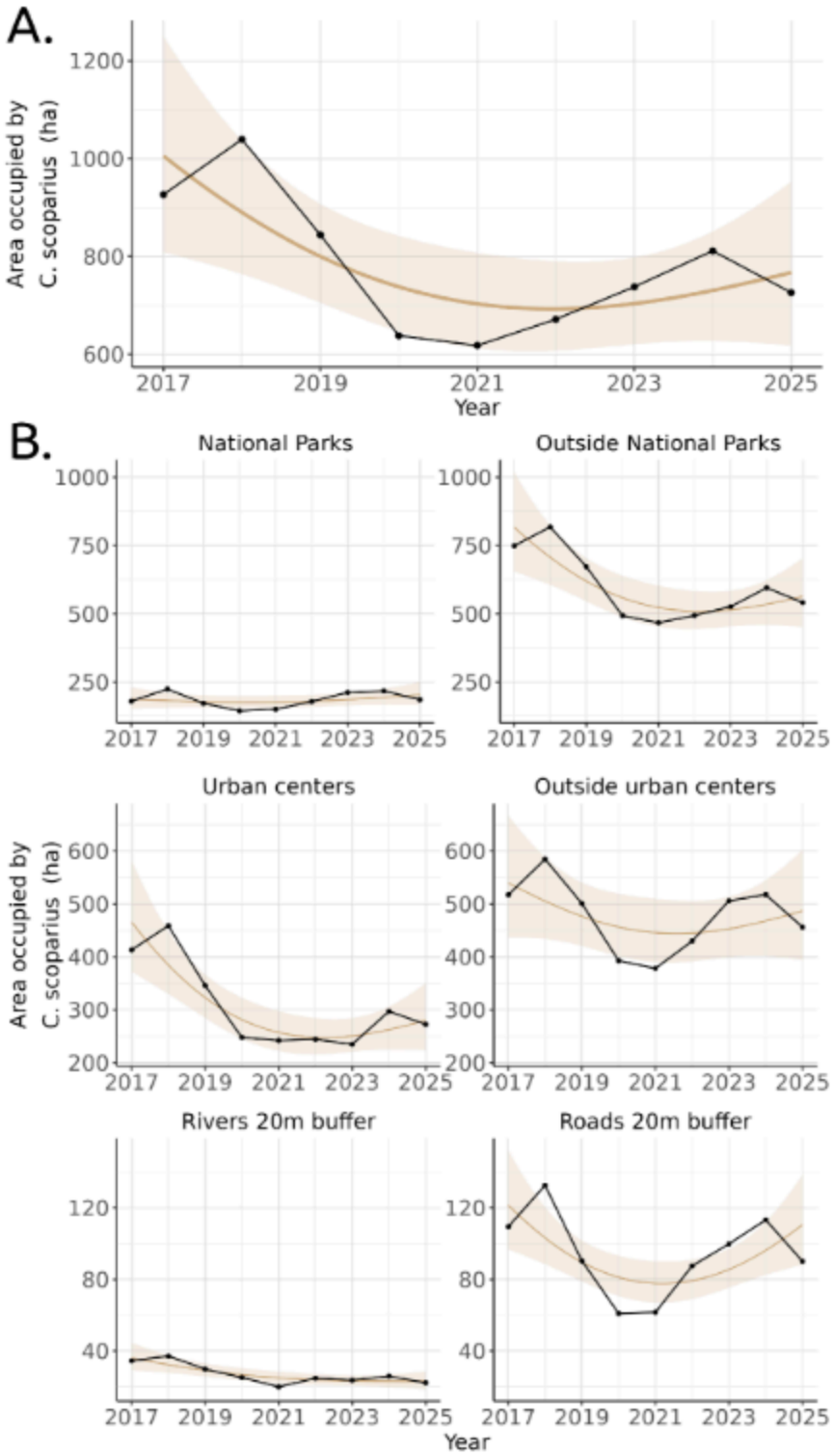


Figure 2

A. Area (ha) occupied by *C. scoparius* in the study area across the analyzed years. B. Details of the area (ha) occupied by *C. scoparius* in the study area across the analyzed years, separated by subarea type. Black points show the random forest classification of the invaded area for each year. Color lines and envelopes indicate the invaded area estimated mean and its corresponding 95 % CI.

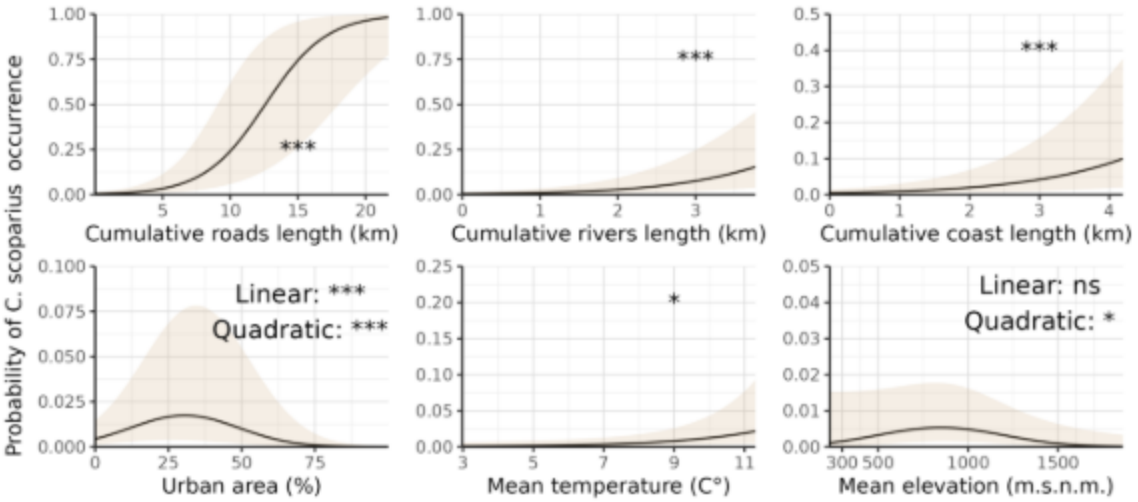


Figure 3

Marginal effects of model parameters on the probability of *C. scoparius* occurrence in a 1km^2 cell. Only significant parameters are shown and keeping all other variables constant at their average. Lines and color envelopes indicate the mean and its corresponding 95 % CI. **Note:** The model was fitted using all occurrence records but only a representative subset of available control cells. Therefore, the predicted probabilities should not be interpreted as estimates of the true occurrence probability in the landscape. However, the shape and direction of the relationships between predictors and occurrence are not affected by this sampling design.

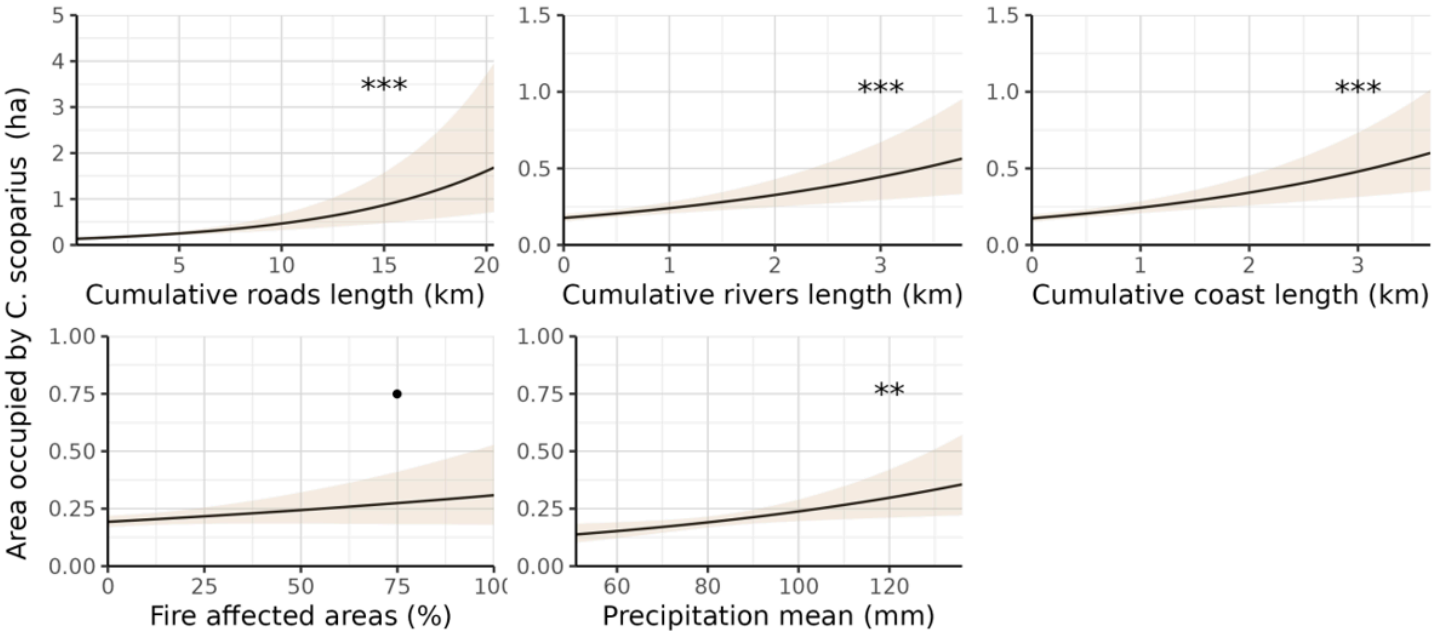


Figure 4

Marginal effects of model parameters of *C. scoparius* invaded area in a 1km^2  cell. Only significant parameters are shown and keeping all other variables constant at their average. In all cases, lines and color envelopes indicate the mean and its corresponding 95 % CI. The statistical significance is indicated (•p ≈ 0.051, *p < 0.05, ** p < 0.01, *** p < 0.001).

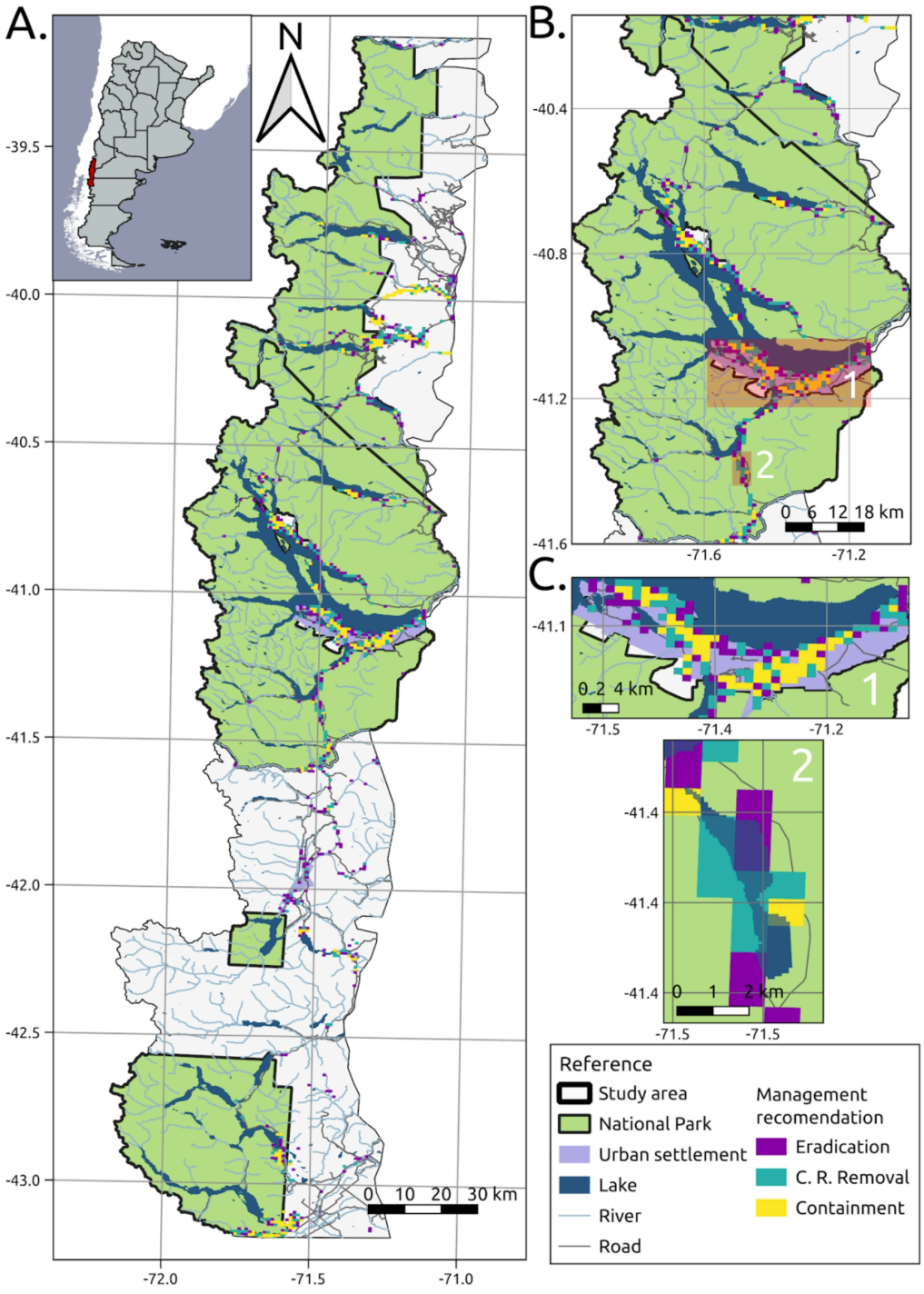


Figure 5

A. Recommended management strategies (*Eradication*, *Complete Reproductive Removal*, *Containment*) for C. scoparius invasion in 1-km² grid cells across the study area for the average of the three last years sampled (2023, 2024, 2025). **B.** Detail of Nahuel Huapi National Park showing two subareas: **(1)** the urban area of San Carlos de Bariloche and **(2)** a non-urbanized area surrounding Lake Guillelmo.

Supplementary Files

This is a list of supplementary files associated with this preprint. Click to download.

- 1SupplementaryMaterial.docx